Available online at www.sciencedirect.com

ScienceDirect

Nuclear Physics B 967 (2021) 115422

NUCLEAR PHYSICS B

www.elsevier.com/locate/nuclphysb

Boundary effects on finite-size scaling for the 5-dimensional Ising model

P.H. Lundow

Department of Mathematics and Mathematical Statistics, Umeå University, SE-901 87 Umeå, Sweden

Received 17 March 2021; accepted 25 April 2021
Available online 28 April 2021
Editor: Hubert Saleur

Abstract

High-dimensional ($d \geq 5$) Ising systems have mean-field critical exponents. However, at the critical temperature the finite-size scaling of the susceptibility χ depends on the boundary conditions. A system with periodic boundary conditions then has $\chi \propto L^{5/2}$. Deleting the $5L^4$ boundary edges we receive a system with free boundary conditions and now $\chi \propto L^2$. In the present work we find that deleting the L^4 boundary edges along just one direction is enough to have the scaling $\chi \propto L^2$. It also appears that deleting L^3 boundary edges results in an intermediate scaling, here estimated to $\chi \propto L^{2.275}$. We also study how the energy and magnetisation distributions change when deleting boundary edges.

1. Introduction

The 5-dimensional (5D) Ising model is well-known to have mean-field critical exponents so that, for example, $\alpha = 0$, $\gamma = 1$ and $\nu = 1/2$. Assuming the usual finite-size scaling (FSS) rules this would imply that the susceptibility scales as $\chi \propto L^{\gamma/\nu} = L^2$ near the critical point β_c, where L is the linear order of the system. However, since we are above the upper critical dimension 4 this rule breaks down and we find instead $\chi \propto L^{d/2} = L^{5/2}$ [1–4], at least for periodic (cyclic) boundary conditions (PBC).

Already in Ref. [5] was it suggested on theoretical, if non-rigorous, grounds that for free boundary conditions (FBC) the rule $\chi \propto L^2$ holds, for $d \geq 5$. This was ultimately settled in

E-mail address: per.hakan.lundow@math.umu.se.

https://doi.org/10.1016/j.nuclphysb.2021.115422

Ref. [6] by rigorous means (under some mild assumptions), after a fruitful debate [7–10]. However, this only concerned the critical point β_c and it is still open whether $\chi \propto L^{5/2}$ for some L-dependent point $\beta(L)$ [11,12].

In the present work we investigate the effect of boundary conditions between FBC and PBC. We thus start with a PBC-system and delete, for example, all boundary edges along one or more, say r, dimensions. This means we delete rL^4 edges and, as we will see, this is enough to change the scaling behaviour of χ to that typical of an FBC-system. Other scenarios for removing boundary edges are also interesting. Deleting rL^3 edges seems to give a scaling behaviour between that of PBC and FBC, suggesting $\chi \propto L^{2.275}$. However, deleting only rL^2 edges gives a scaling behaviour indistinguishable from that of PBC.

We will study the behaviour of not only the susceptibility, but also the distribution shape (kurtosis) and the effects on the energy distribution (variance, skewness and kurtosis). However, though we have collected data for a wide range of system sizes (up to $L = 95$) our investigation only takes place at the critical point.

2. Definitions and details

The underlying graph is the $L \times L \times L \times L \times L$ grid graph on $N = L^5$ vertices but with different cases of boundary conditions, to be defined below. With each vertex i we associate a spin $s_i = \pm 1$ and let the Hamiltonian be $\mathscr{H} = \sum_{ij} s_i s_j$. The magnetisation of a state $s = (s_1, \ldots, s_N)$ is $M = \sum_i s_i$, where we sum over the vertices i, and the energy is $E = \sum_{ij} s_i s_j$, where we sum over the edges ij. Their normalised forms are denoted $m = M/N$ and $U = E/N$. As usual, $\langle \ldots \rangle$ denotes the thermal-equilibrium mean and $\mathrm{var}(\ldots)$ the variance. Quantities of interest to us are the susceptibility $\chi = \langle M^2 \rangle / N$, the internal energy $\mathcal{U} = \langle E \rangle / N$ and the specific heat $\mathcal{C} = \mathrm{var}(E)/N$ (we ignore the usual β^2-factor). Distribution shape characteristics such as skewness and kurtosis are also of interest. Since the distribution of magnetisations is symmetric (hence skewness zero) when no external field is present, only its kurtosis is considered:

$$\mathcal{K} = \frac{\langle M^4 \rangle}{\langle M^2 \rangle^2} \tag{1}$$

For the energy distribution its skewness is defined as

$$\mathcal{S} = \frac{\langle (E - \langle E \rangle)^3 \rangle}{\mathrm{var}(E)^{3/2}} \tag{2}$$

and its kurtosis as

$$\mathcal{K} = \frac{\langle (E - \langle E \rangle)^4 \rangle}{\mathrm{var}(E)^2} \tag{3}$$

Hopefully the context will make it clear whether $\mathcal{K}$ is referring to energy or magnetisation kurtosis.

We have collected data for systems of linear order $L = 15$, 19, 23, 31, 39, 47, 55, 63, 71, 79, 87 and 95 using standard Wolff-cluster updating [13]. An expected N spins were flipped between measurements of energy and magnetisations. All sampling took place at the critical point $\beta_c = 0.11391498$ [14]. The number of sample n_s are between 100000 and 200000 for $15 \le L \le 63$ and ca 50000 for $71 \le L \le 95$. However, for PBC we have at least 500000 samples for $15 \le L \le 79$ and 50000 for $L = 87, 95$. Error bars of the quantities mentioned above are estimated from bootstrap resampling of the data.

The vertices of our graph are the integer points in a 5D system, $V = \{(i_1, \ldots, i_5) : 1 \leq i_1, \ldots, i_5 \leq L\}$. We let E denote the edges of a PBC-system, which has $5L^5$ edges. There are two types of edges, the bulk edges and the boundary edges. The bulk edges are those edges $e = \{i, j\}$, where $i = (i_1, \ldots, i_5)$ and $j = (j_1, \ldots, j_5)$, such that the Manhattan distance $\sum_{r=1}^{5} |i_r - j_r|$ (sum over coordinates) is 1. The boundary edges belong to one of five sets, $D_1, \ldots, D_5$. For example, the boundary edges in D_1 are on the form

$$e = \{(1, i_2, i_3, i_4, i_5), (L, i_2, i_3, i_4, i_5)\}, \tag{4}$$

where $1 \leq i_2, i_3, i_4, i_5 \leq L$. Hence there are L^4 such edges in D_1. In general, the set D_r has the 1 and L at coordinate r, for $1 \leq r \leq 5$. For convenience we define $C_r = D_1 \cup \ldots \cup D_r$, so that $|C_r| = rL^4$. Thus the FBC-system only keeps the bulk edges, $E \setminus C_5$, which then has cardinality $5L^5 - 5L^4$.

We will now define two subsets of D_1. The set of edges on the form

$$e = \{(1, i_2, i_3, i_4, x), (L, i_2, i_3, i_4, x)\}, \tag{5}$$

where $1 \leq x \leq r$, is denoted B_r and contains rL^3 edges. The set of edges on the form

$$e = \{(1, i_2, i_3, x, y), (L, i_2, i_3, x, y)\}, \tag{6}$$

where $1 \leq x, y \leq r$, is denoted A_r and contains r^2L^2 edges.

We have collected measurements of energy and magnetisation for the following boundary cases: E (or PBC, deleting no edges), $E \setminus A_r$ (deleting r^2L^2 edges, $r = 1, 2, 4$), $E \setminus B_r$ (deleting rL^3 edges, $r = 1, 2, 4$), $E \setminus C_r$ (deleting rL^4 edges, $r = 1, 2, 3, 4, 5$, where $r = 5$ is FBC). However, for short we will usually refer to these cases as simply PBC, A_r, B_r and C_r, with C_5 synonymous to FBC.

One could of course also consider other interesting cases by letting the parameter r depend weakly on L, but presumably it would require rather large L to tell a new scaling effect from an extra correction term. An alternative, in the cases A_r and B_r, is to let the x and y be centred around $L/2$ instead of its current choice $1 \leq x, y \leq r$.

3. Scaling of susceptibility

As we mentioned above we have $\chi \propto L^{5/2}$ for PBC and $\chi \propto L^2$ for FBC (C_5). Here we will see that $\chi \propto L^{5/2}$ in the A_r-case, $\chi \propto L^2$ in the C_r-case, but $\chi \propto L^{2.275}$ for the inbetween case B_r.

We begin by taking our data points, χ/L^a versus $1/L$, and fit a line $y = c_0 + c_1 x$ to these, for each boundary case. Testing a range of exponents a between 2 and 5/2 we compute the root-mean-square (RMS) of the deviation between the fitted line and the points. A minimum RMS then indicates the optimal value of a. This ignores any higher-order corrections but this, as we will see, appears quite acceptable. Since we know the correct values of a for PBC ($a = 2.5$) and FBC ($a = 2$) this also gives us an indication of the error in our estimate.

In Fig. 1 we see that PBC and A_r prefer exponents a near 5/2, with minimum at 2.475 (PBC), 2.49 (A_1), 2.50 (A_2) and 2.535 (A_4). This gives the estimate $a = 2.500(25)$. Deleting a few of the points in the fit will of course give slightly different results, but within the error bar.

Continuing with the B_r-case we show RMS versus a in Fig. 2. The mean of the minima centre around 2.275(10), where we have used $L \geq 23$ for the fitted line. It would perhaps be natural to

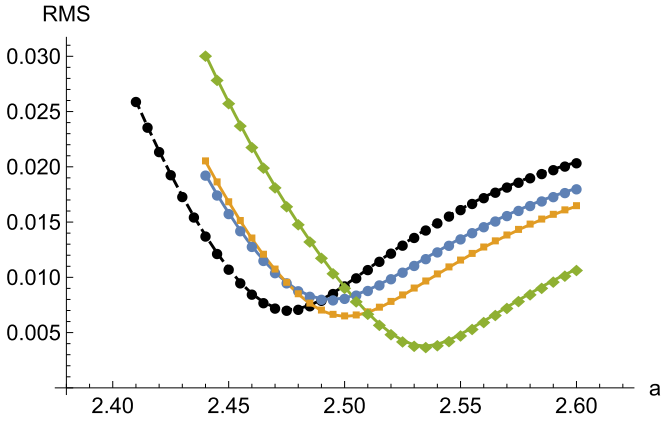

Fig. 1. (Colour on-line) Root-mean-square of linear fit to points $(1/L, \chi/L^a)$ plotted versus a for PBC (black), A_1 (blue), A_2 (orange) and A_4 (green). Minimum at respectively 2.475, 2.49, 2.50, 2.535.

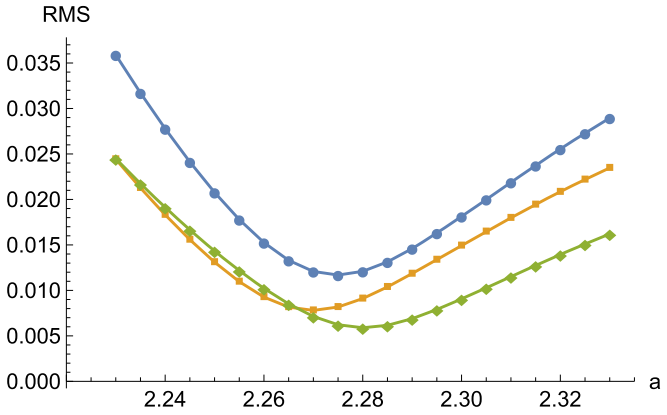

Fig. 2. (Colour on-line) Root-mean-square of linear fit to points $(1/L, \chi/L^a)$ plotted versus a for B_1 (blue), B_2 (orange) and B_4 (green). Minimum at 2.275, 2.27, 2.28, respectively.

expect the linear fit to favour the mid-point 2.25 between 2 and 2.5 but this is not supported by the present data. It should be remarked that, the mean value of the minima is remarkably stable between different point sets but the individual minima vary between 2.255 and 2.29. Hence we suggest that the correct a-value is a little larger than 2.25.

Finally, the case of C_r (thus including FBC) is shown in Fig. 3. The RMS-plots clearly prefer an exponent close to 2. With the present linear fit, using $L \geq 19$, we find an average minimum 2.00(1). Trying different point sets gives almost the same average but individual minima varies between 1.97 and 2.015.

In Figs. 4, 5 and 6 we show the normalised susceptibility χ/L^a versus $1/L$ together with the fitted lines $y = c_0 + c_1 x$ from which we read the asymptotic value c_0. This very simple rule appears quite sufficient and we see no presence of any higher-order correction terms. In fact, plotting $c_1 = L(\chi/L^a - c_0)$ versus $1/L$ is effectively constant (modulo noise, increasing with L). We show here only the case of B_r in Fig. 7 but the other cases results in quite similar plots.

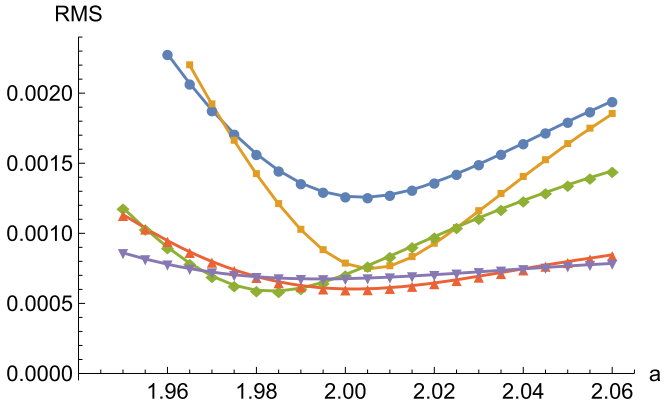

Fig. 3. (Colour on-line) Root-mean-square of linear fit to points $(1/L, \chi/L^a)$ plotted versus a for C_1 (blue, values divided by 3), C_2 (orange), C_3 (green), C_4 (red) and C_5 (purple). Minimum at respectively 2.005, 2.005, 1.985, 2.000, 1.995.

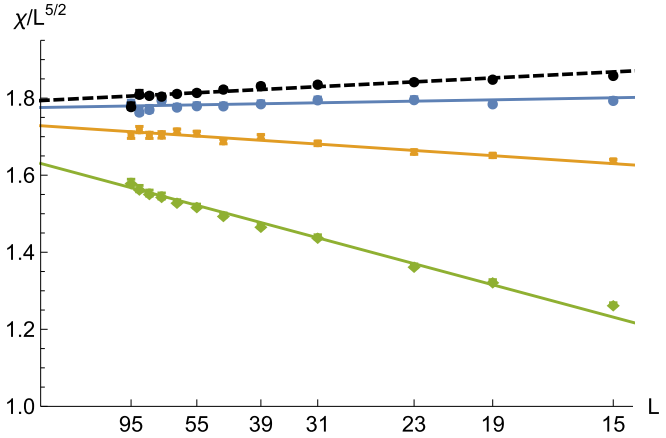

Fig. 4. (Colour on-line) Normalised susceptibility $\chi/L^{5/2}$ versus $1/L$ for $L = 15, 19, 23, 31, 39, 47, 55, 63, 71, 79, 87$ and 95. Cases are PBC (black), A_1 (blue), A_2 (orange) and A_4 (green). Fitted lines are, respectively, $y = 1.794 + 1.11x$, $y = 1.775 + 0.40x$, $y = 1.729 - 1.50x$, $y = 1.630 - 6.0x$ where $x = 1/L$.

4. Magnetisation distribution

We will here make an attempt to describe the distribution of the magnetisation. Beginning with the kurtosis $\mathcal{K}$ for PBC we expect it to take the asymptotic value $\Gamma(1/4)^4/(8\pi^2) \approx 2.1884$ [1] and for FBC we expect it to be 3, as is characteristic for a normal distribution.

In general the mean-field density function [1,2]

$$f(x) = c_0 \exp(-c_2 x^2 - c_4 x^4) \tag{7}$$

fits these distributions very well, except for very small systems where a correction factor is needed. Note that the case $c_2 = 0$ gives the kurtosis 2.1884 mentioned above for all $c_4 > 0$. The distribution then is unimodal when $c_2 > 0$ giving $\mathcal{K} > 2.1884$ and a bimodal distribution

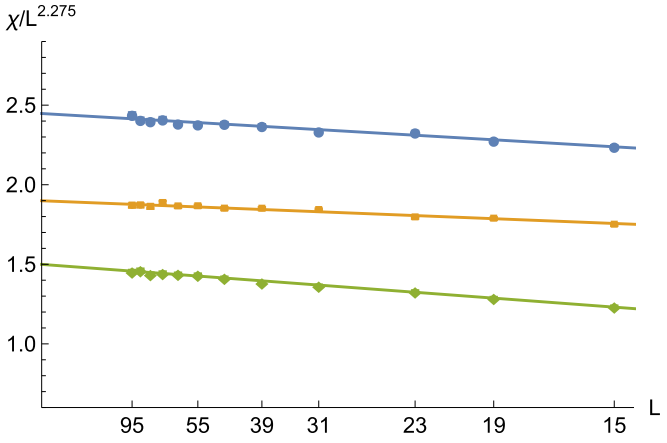

Fig. 5. (Colour on-line) Normalised susceptibility $\chi/L^{2.275}$ versus $1/L$ for $L = 15, 19, 23, 31, 39, 47, 55, 63, 71, 79, 87$ and 95. Cases are B_1 (blue), B_2 (orange) and B_4 (green). Fitted lines are, respectively, $y = 2.45 - 3.1x$, $y = 1.90 - 2.2x$, $1.50 - 4.0x$ where $x = 1/L$.

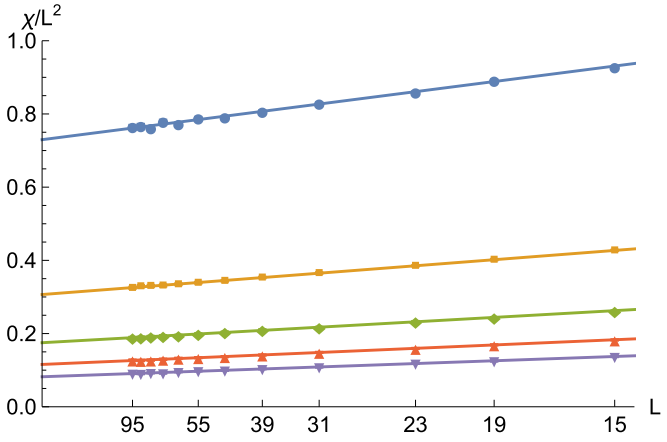

Fig. 6. (Colour on-line) Normalised susceptibility χ/L^2 versus $1/L$ for $L = 15, 19, 23, 31, 39, 47, 55, 63, 71, 79, 87$ and 95. Cases are (downwards) C_1 (blue), C_2 (orange), C_3 (green), C_4 (red) and C_5 (purple). Fitted lines are, respectively, $y = 0.730 + 3.0x$, $y = 0.307 + 1.8x$, $0.175 + 1.3x$, $y = 0.116 + 1.0x$, $y = 0.082 + 0.83x$ where $x = 1/L$.

when $c_2 < 0$ corresponding to $\mathcal{K} < 2.1884$. The function $f(x)$ can now be determined from the variance and the kurtosis. We will here only show the standardised form (variance 1).

The kurtosis plotted in Fig. 8 demonstrate an interesting feature with regard to the distribution shape. Since the cases PBC and A_1 all have $\mathcal{K} < 2.1884$ they are thus bimodal but converge to a "flat" distribution ($c_2 = 0$). However, in the case of A_2 the kurtosis is almost constant ≈ 2.2 for all L, just barely unimodal. For A_4 we are safely into unimodal territory though.

In Fig. 9 we show an example of a standardised distribution in the A_2-case for $L = 63$. Based on the kurtosis we find the density function $f(x)$ numerically. Here $\mathcal{K} = 2.1922$ which gives $f(x) = 0.3213\exp(-0.004541x^2 - 0.1130x^4)$, where $x = M/\sigma$. A Pearson goodness-of-fit test is now used to see if we should reject the hypothesis that $f(x)$ fits the magnetisation distribution.

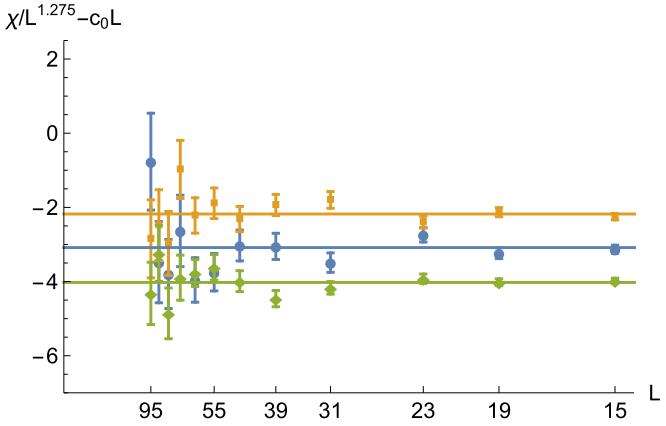

Fig. 7. (Colour on-line) $L(\chi/L^{2.275} - c_0)$ versus $1/L$ for $L = 15, 19, 23, 31, 39, 47, 55, 63, 71, 79, 87$ and 95. Cases are B_1 (blue), B_2 (orange) and B_4 (green). Values of c_0 are, respectively, 2.45, 1.90, 1.50. Constant lines are, respectively, $y = -3.1$, $y = -2.2$, $y = -4.0$. See Fig. 5.

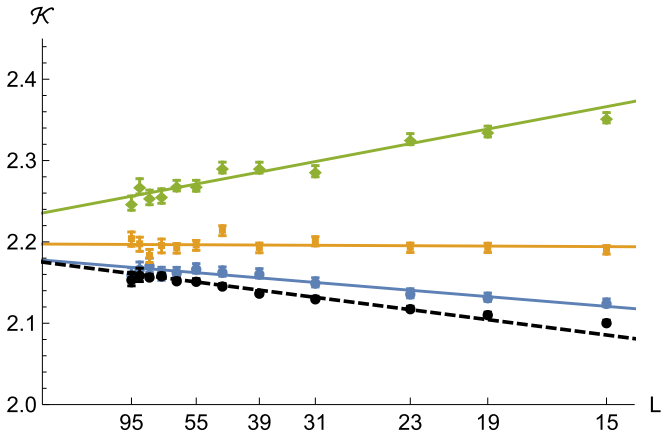

Fig. 8. (Colour on-line) Magnetisation kurtosis $\mathcal{K}(\beta_c)$ versus L for $L = 15, 19, 23, 31, 39, 47, 55, 63, 71, 79, 87$ and 95. Cases are, PBC (black, dashed curve), A_1 (blue), A_2 (orange) and A_4 (green). Lines fitted to $L \geq 19$ give asymptotic values, respectively, 2.18(1), 2.18(1), 2.20(1), 2.24(1).

In fact we find $\chi^2/\text{dof} \approx 0.96$ for dof $= 200$ and a p-value of 0.61 so we choose not to reject this.

This was repeated for the other cases (three A_r) and sizes (twelve L) as well, using $\lceil 2n_s^{2/5} \rceil$ equiprobable bins (Mathematica's default) for n_s samples. Median p-value over these 36 instances is 0.50 with interquartile range 0.47 and all were larger than 0.05. The hypothesis that the distribution is described by Eq. (7) is thus not rejected for A_r and $L \geq 15$.

Moving on to the case B_r we show the magnetisation kurtosis in Fig. 10 and it does not appear to converge to 3 for any of these cases. The distributions still fit Eq. (7) though. The Pearson test gave the median p-value 0.71 and an interquartile range of 0.48 and only one of the 36 instances ($r = 1$, $L = 55$) gave $p < 0.05$. Since 5% of the instances will fail even if the hypothesis is true we find this quite normal. We thus do not reject that Eq. (7) fits these distributions for B_r and $L \geq 15$. In Fig. 11 we show an example of this distribution and $f(x)$ for B_1 and $L = 63$.

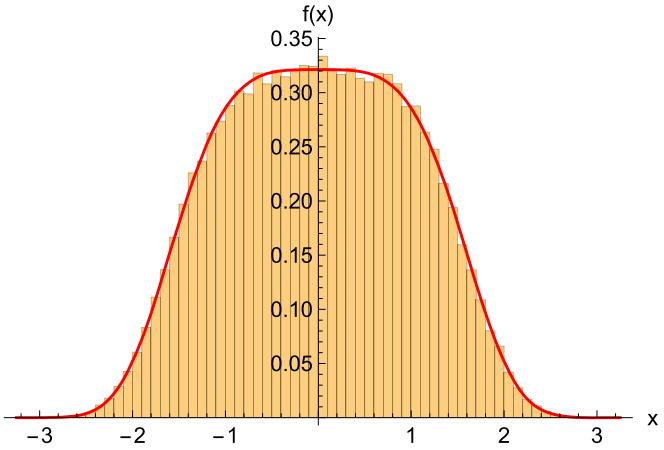

Fig. 9. (Colour on-line) Standardised magnetisation distribution density for A_2-case, $L = 63$. Kurtosis $\mathcal{K} = 2.192(6)$ gives $f(x) = 0.3213\exp(-0.00445x^2 - 0.113x^4)$ (red curve) where $x = M/\sigma$. A Pearson goodness-of-fit test is passed with p-value 0.61.

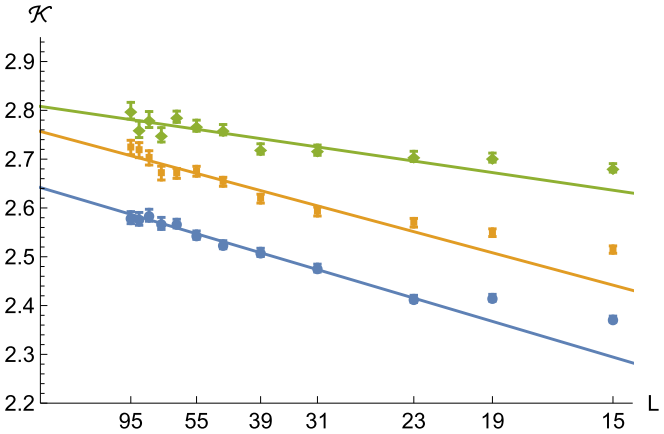

Fig. 10. (Colour on-line) Magnetisation kurtosis $\mathcal{K}(\beta_c)$ versus L for $L = 15$, 19, 23, 31, 39, 47, 55, 63, 71, 79, 87 and 95. Cases are B_1 (blue), B_2 (orange) and B_4 (green). Lines fitted to $L \geq 23$ give asymptotic values, respectively, 2.64(1), 2.76(1), 2.81(1).

For the C_r-case the kurtosis is close to 3 (modulo noise) in almost all instances. Only for $r = 1$ do we see a weak trend with values clearly distinct from 3 for the smallest L (no figure). We tested the hypothesis that the distribution of the magnetisation samples are Gaussian for all r and $L \geq 23$. Indeed, of these 50 instances only 4 (8%) fail (p-value less than 0.05) which is to be expected. The median p-value over the instances was 0.46 with interquartile range 0.45. Thus we do not reject the hypothesis.

5. Scaling of energy quantities

Let us first discuss the finite-size scaling of the internal energy $\mathcal{U}$. Across the different cases the data seem to agree on the common limit energy $\mathcal{U}(\beta_c) = 0.6756(1)$. For PBC a very simple

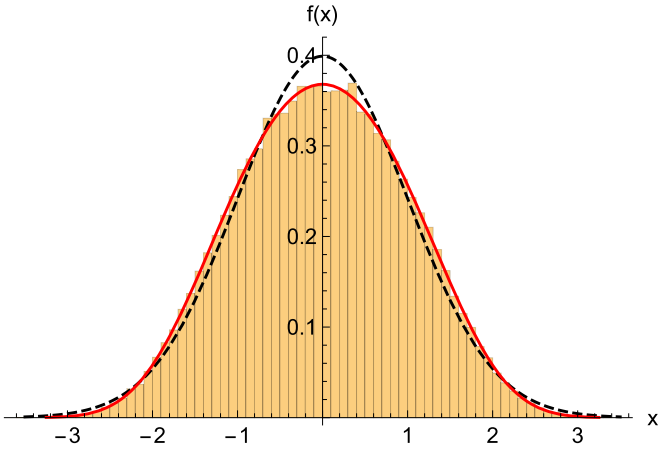

Fig. 11. (Colour on-line) Standardised magnetisation distribution density for $L = 63$ with edges B_1. Kurtosis $\mathcal{K} = 2.568(9)$ gives $f(x) = 0.3680\exp(-0.327x^2 - 0.0338x^4)$ (red curve) where $x = M/\sigma$. Dashed black curve is density of a normal distribution. A Pearson goodness-of-fit test is passed with p-value 0.80.

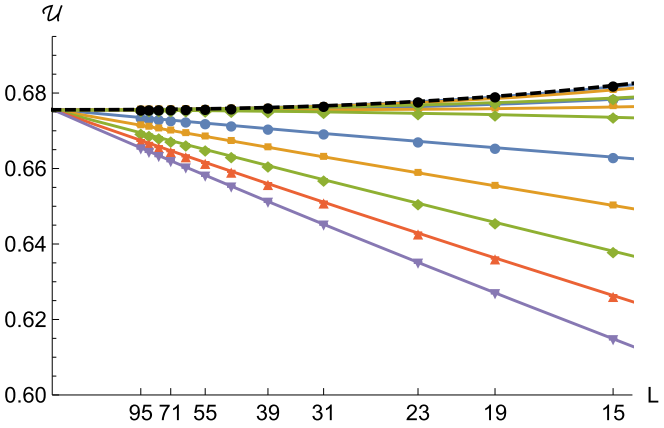

Fig. 12. (Colour on-line) Energy $\mathcal{U}$ versus L for $L = 15$, 19, 23, 31, 39, 47, 55, 63, 71, 79, 87 and 95. Boundary conditions are (downwards) PBC (black, dashed curve), A_r $(r = 1, 2, 4)$, B_r $(r = 1, 2, 4)$ and C_r $(r = 1, \ldots, 5)$. The fitted curves (see text) have the common limit 0.6756(1). Error bars are shown but smaller than the points.

scaling rule $\mathcal{U}_L = c_0 + c_1/L^{5/2}$ is sufficient. For A_r we suggest $\mathcal{U}_L = c_0 + c_1/L^{5/2} + c_2/L^5$, though the choice of the second exponent is uncertain.

At the other end of the spectrum, for FBC and C_r, the rule $\mathcal{U}_L = c_0 + c_1/L + c_2/L^{3/2}$ gives stable scaling, also used in Ref. [8]. For B_r the rule $\mathcal{U}_L = c_0 + c_1/L + c_2/L^{5/2}$ gives stable behaviour when deleting points. These scaling rules give the limit value $c_0 = 0.6756(1)$ above but we seem unable to provide any more digits. Needless to say, we have no theory-based support for these scaling rules. In Fig. 12 we plot the energy versus $1/L$ for all cases and sizes together with fitted curves as just described.

Since the specific heat is bounded for 5D systems [15] one might expect its finite-size scaling to be similar to that of the energy. Unfortunately the scaling rules above do not seem to apply

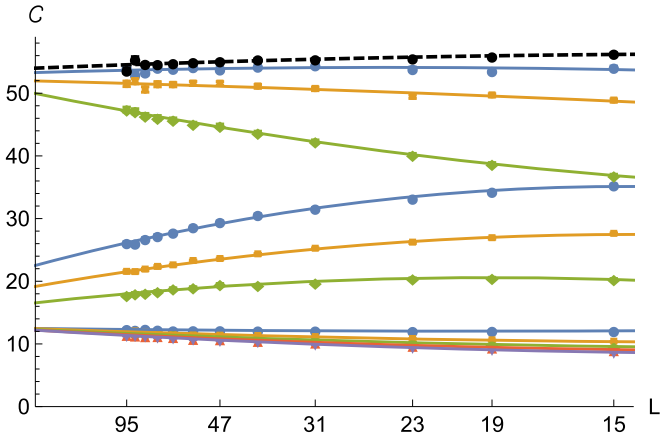

Fig. 13. (Colour on-line) Specific heat $\mathcal{C}$ versus L for $L = 15, 19, 23, 31, 39, 47, 55, 63, 71, 79, 87$ and 95. Boundary conditions are (downwards at y-axis) PBC (black, dashed curve), A_r $(r = 1, 2, 4)$, B_r $(r = 1, 2, 4)$ and C_r $(r = 1, \ldots, 5)$. Limit values range from 54 for PBC to 12.5 for FBC (see text). Error bars are shown but smaller than the points.

to the specific heat. In Fig. 13 we therefore plot the specific heat together with fitted 2nd degree polynomials which at least provides rough estimates of the limit values.

For PBC we estimate the limit $\mathcal{C}(\beta_c) \approx 54.0(5)$ (marginally less than in Ref. [14]). In the A_r-case we obtain the limits 53.0(5), 52.0(5), 50.0(5) for $r = 1, 2, 4$, respectively. The B_r-case gives 22.5(5), 19.0(5), 16.5(5) for $r = 1, 2, 4$, respectively. Finally, the C_r-case resulted in the (probably) common estimate 12.5(5), though the noise is larger than the differences between the estimated limits.

In Ref. [8] only one correction term was used with exponent 1/3 for FBC, so that $\mathcal{C}_L = c_0 + c_1/L^{1/3}$. All C_r-instances are indeed well-fitted by this elegant rule, but this would lead to a limit of 14.7 for C_5 (FBC), larger than the resulting limit 12.6 for C_1. Hence, we hesitate to use this simple rule since all data suggest that the specific heat should decrease when deleting boundary edges, just like the energy does in Fig. 12.

In Fig. 14 we see the effect that the boundary has on the skewness of the energy distribution. At the top of the figure we see that PBC and A_r are almost indistinguishable and they all agree on a common limit value of 1.023(5) based on fitted lines. For PBC and A_1 the skewness is effectively constant (modulo noise) over L. There is only a very small size-dependence for A_2 and A_4.

For B_r the skewness has clearly separated itself from PBC. Also, the size-dependence becomes clearly nonlinear. Fitting 2nd degree polynomials to the points we estimate the limits 0.72(1), 0.50(1) and 0.31(1) for $r = 1, 2, 4$ respectively (error bars from deleting one point in the fit). In the C_r-case the skewness is practically zero for all L for $r = 2, 3, 4, 5$ but there is a distinct (almost) linear size-dependence for $r = 1$, becoming effectively zero for $L \geq 47$.

The kurtosis $\mathcal{K}$ of the energy distribution is shown in Fig. 15. At this point the pattern is clear. PBC and A_r behave similarly (dashed curves in the figure), though A_4 stands out, with limit values 4.48(1) (PBC), 4.39(4) $(r = 1)$, 4.56(3) $(r = 2)$ and 4.46(3) $(r = 4)$, with error bars estimated by removing one point at a time from a fitted 2nd degree polynomial. Since the error bars are larger for A_r they could in fact have a common limit value 4.48. In Fig. 16 we show the energy distribution for PBC $(L = 79)$, which is quite similar to that of A_r.

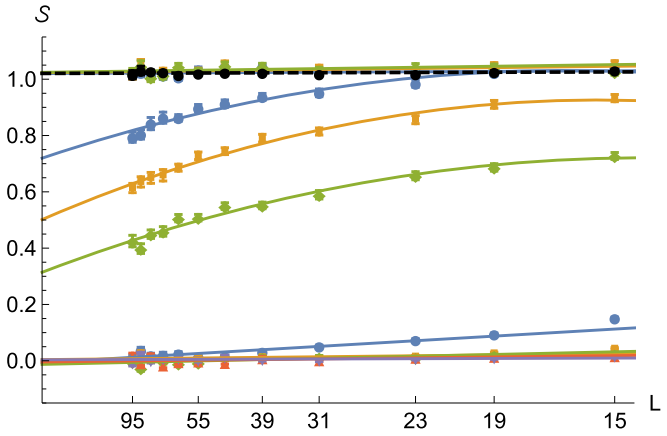

Fig. 14. (Colour on-line) Energy skewness $\mathcal{S}$ versus L for $L = 15, 19, 23, 31, 39, 47, 55, 63, 71, 79, 87$ and 95. Boundary conditions are: at the top, PBC (black, dashed curve) and A_r ($r = 1, 2, 4$, indistinguishable); middle three, B_r ($r = 1, 2, 4$ downwards); at the bottom, C_r ($r = 1, \ldots, 5$, with $r = 1$ deviating). Limit values range from 1.02 for PBC and A_r to 0 for FBC (see text for details). Error bars are shown but often smaller than the points.

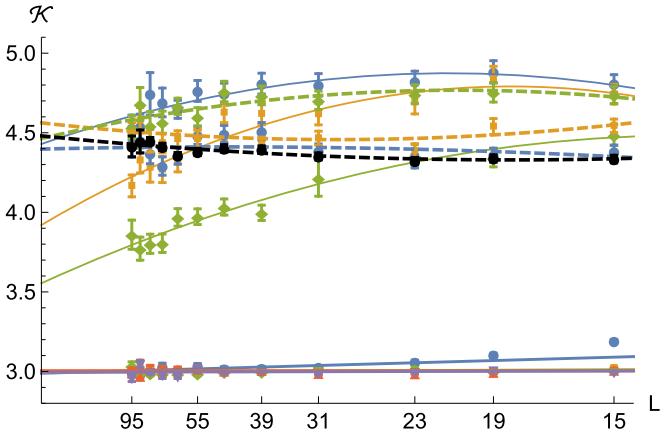

Fig. 15. (Colour on-line) Energy kurtosis $\mathcal{K}$ versus L for $L = 15, 19, 23, 31, 39, 47, 55, 63, 71, 79, 87$ and 95. Boundary conditions are: at the top, PBC (black, dashed curve) and A_r ($r = 1, 2, 4$, (blue, orange, green; dashed curves); B_r ($r = 1, 2, 4$ blue, orange, green; solid curves); at the bottom, C_r ($r = 1, \ldots, 5$, with $r = 1$ deviating). See text for limit values. Error bars are shown but sometimes smaller than the points.

For B_r (solid curves in figure) we estimate the limits 4.43(3) ($r = 1$), 3.93(3) ($r = 2$) and 3.55(3) ($r = 4$) from fitted 2nd degree polynomials. Possibly the $r = 1$-case has the same limit value as PBC. The C_r-case all favour the estimate 3.00(1) by way of fitted lines, but there is a small size dependence for $r = 1$.

We performed a Pearson goodness-of-fit test to compare the energy distributions of C_r to a Gaussian distribution. For $r = 2, \ldots, 5$, this test is passed for all $L \geq 31$, giving a median p-value of 0.47 and interquartile range 0.34 over the 36 instances. However, for $r = 1$ we need $L \geq 63$ to pass the test on the 5%-level.

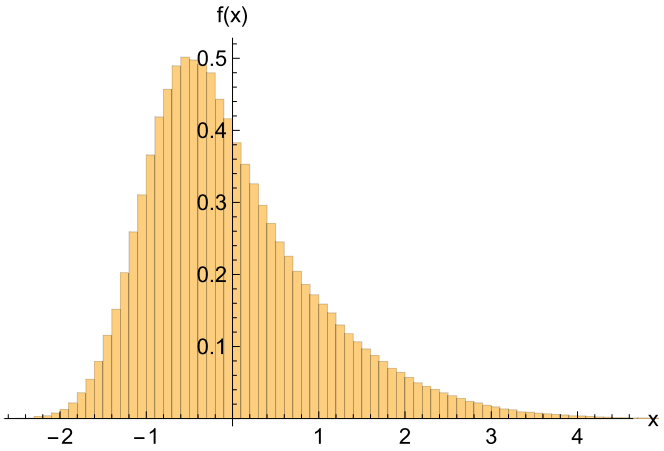

Fig. 16. (Colour on-line) Standardised energy distribution density for PBC, $L = 79$, $n_s = 500000$. This instance has energy $\mathcal{U} = 0.6756$, specific heat $\mathcal{C} = 54.7$, skewness $\mathcal{S} = 1.03$ and kurtosis $\mathcal{K} = 4.44$. Note that $x = (E - \langle E \rangle)/\sqrt{\mathrm{var}\,(E)}$.

6. Conclusion

We have investigated several scenarios of deleting boundary edges from a PBC-system, where an FBC-system corresponds to deleting $5L^4$ edges. For example, what happens to the finite-size scaling of the susceptibility when we delete all boundary edges in only one direction, i.e., L^4 edges? Remarkably, we find that this is enough to switch the scaling behaviour to that associated with FBC. The distribution of magnetisations, essentially distributed as $c_0 \exp(-c_4 x^4)$ for PBC, has also switched to Gaussian for $L \geq 23$, to the extent that it passes a Pearson goodness-of-fit test.

Deleting just L^2 boundary edges does not change the scaling behaviour significantly from that of PBC though it does increase the kurtosis slightly, making the distribution of magnetisations unimodal. However, deleting L^3 boundary edges changes the susceptibility scaling to something strictly inbetween PBC and FBC, we estimate that $\chi \propto L^{2.275}$.

We also note that all magnetisation distributions are well-fitted by the simple formula in Eq. (7), passing a Pearson test to the expected degree.

The energy-related quantities also change when deleting boundary edges, though correction-to-scaling terms give less than clear scaling rules. We suggest that deleting rL^4 edges (C_r-case) may all give the same specific heat limit value of 12.5(5), for $r = 1, \ldots, 5$. Deleting just rL^2 edges, and for that matter, rL^3 edges, gives us specific heat values inbetween PBC and FBC.

The energy skewness is essentially the same for PBC and when deleting rL^2 edges, $\mathcal{S} \to 1.02$. Deleting rL^4 edges gives $\mathcal{S} \to 0$. Deleting rL^3 edges gives limit values inbetween these two.

The energy kurtosis for PBC and when deleting rL^2 edges may have the same limit value, say 4.5, but there is too much noise to say with any certainty. Deleting rL^4 puts the kurtosis close to 3 and, as we may expect, a Pearson test suggests the energy distribution is essentially Gaussian in this case, if L is large enough. However, deleting rL^3 edges puts the kurtosis somewhere inbetween, possibly $r = 1$ may give the same limit as PBC.

One may well wonder how this generalises to higher dimensions. For example, starting with a 6D system with periodic boundary conditions we expect the finite-size scaling $\chi \propto L^3$. If we delete the L^5 boundary edges along one direction, is this enough to change the scaling to $\chi \propto L^2$? What happens when we delete L^4, L^3, L^2 edges?

CRediT authorship contribution statement

P.H. Lundow: Investigation, Conceptualization, Methodology, Software, Data curation, Writing Original draft preparation, Reviewing, Editing, Visualization.

Declaration of competing interest

The authors declare that they have no known competing financial interests or personal relationships that could have appeared to influence the work reported in this paper.

Acknowledgements

The computations were performed on resources provided by the Swedish National Infrastructure for Computing (SNIC) at Chalmers Centre for Computational Science and Engineering (C3SE).

References

[1] E. Brezin, J. Zinn-Justin, Nucl. Phys. B 257 (1985) 867.
[2] K. Binder, M. Nauenberg, V. Privman, A.P. Young, Phys. Rev. B 31 (1985) 1498.
[3] H.W.J. Blöte, E. Luijten, Europhys. Lett. 38 (1997) 565.
[4] E. Luijten, K. Binder, H.W.J. Blöte, Eur. Phys. J. B 9 (1999) 289.
[5] J. Rudnick, G. Gaspari, V. Privman, Phys. Rev. B 32 (1985) 7594.
[6] F. Camia, J. Jiang, C.M. Newman, Probab. Theory Relat. Fields (2021), https://doi.org/10.1007/s00440-021-01041-9.
[7] P.H. Lundow, K. Markström, Nucl. Phys. B 845 (2011) 120.
[8] P.H. Lundow, K. Markström, Nucl. Phys. B 889 (2014) 249.
[9] B. Berche, R. Kenna, J.-C. Walter, Nucl. Phys. B 865 (2012) 115.
[10] E. Flores-Sola, B. Berche, R. Kenna, M. Weigel, Phys. Rev. Lett. 116 (2016) 115701.
[11] M. Wittmann, A.P. Young, Phys. Rev. E 90 (2014) 062137.
[12] P.H. Lundow, K. Markström, Nucl. Phys. B 911 (2016) 163.
[13] U. Wolff, Phys. Rev. Lett. 62 (1989) 361.
[14] P.H. Lundow, K. Markström, Nucl. Phys. B 895 (2015) 305.
[15] A.D. Sokal, Phys. Lett. A 71 (1979) 451.